

**ALUMINUM SITING IN THE ZSM-22 AND THETA-1 ZEOLITES REVISITED: A QM/MM STUDY**

Stepan SKLENAK<sup>a1,\*</sup>, Jiří DĚDEČEK<sup>a2</sup>, Chengbin LI<sup>a3</sup>, Fei GAO<sup>a4</sup>,  
Bavornpon JANSANG<sup>a5</sup>, Bundet BOEKFA<sup>a6</sup>, Blanka WICHTERLOVÁ<sup>a7</sup> and  
Joachim SAUER<sup>b</sup>

<sup>a</sup> J. Heyrovský Institute of Physical Chemistry, Academy of Sciences of the Czech Republic, v.v.i.,  
Dolejškova 3, 182 23 Prague 8, Czech Republic; e-mail: <sup>1</sup> stepan.sklenak@jh-inst.cas.cz,  
<sup>2</sup> dedecek@jh-inst.cas.cz, <sup>3</sup> cbli.wh@gmail.com, <sup>4</sup> fei.gao@jh-inst.cas.cz, <sup>5</sup> bavornpon@yahoo.com,  
<sup>6</sup> g4784002@ku.ac.th, <sup>7</sup> blanka.wichterlova@jh-inst.cas.cz

<sup>b</sup> Institut für Chemie, Humboldt-Universität zu Berlin, Unter den Linden 6, 10099 Berlin,  
Germany; e-mail: sek.qc@chemie.hu-berlin.de

Received May 27, 2008

Accepted July 10, 2008

Published online September 17, 2008

*Dedicated to Professor Rudolf Zahradník on the occasion of his 80th birthday.*

The Al siting in the silicon rich ZSM-22 and Theta-1 zeolites of the TON structure was investigated analyzing already published <sup>27</sup>Al 3Q MAS NMR experimental data using QM/MM calculations. The results of our computations show that Al atoms can be located in 6 framework T positions because the two eightfold sites (T1 and T2) split into four fourfold T sites after an Al/Si substitution. The observed resonance at 55.5 ppm corresponds to the T4 site which is predominantly occupied by Al. This site is not located on the surface of the TON ten-membered ring channel and thus the protonic sites related with the majority of Al atoms in the TON structure exhibit a significantly limited reaction space. The <sup>27</sup>Al NMR signals centered at 57.6 and 58.7 ppm correspond to either the T2 and T3 sites, respectively, or only to T2. The T2 and T3 sites accommodate some 40% and up to 10%, respectively, of Al while the T1 site is unoccupied by Al. Isotropic shifts of 61.1 and 61.6 ppm were calculated for Al atoms located in the T1-1 and T1-2 sites, respectively. The effect of a silanol "nest" as a next-next-nearest neighbor on the <sup>27</sup>Al isotropic chemical shift of Al located in the T4 site is calculated to be less than 1 ppm.

**Keywords:** QM/MM calculations; *Ab initio* calculations; BLYP; GIAO; Zeolites; <sup>27</sup>Al 3Q MAS NMR spectroscopy; ZSM-5 catalyst; Heterogeneous catalysis.

Zeolites are crystalline microporous aluminosilicates widely used as molecular sieves and catalysts in industrial chemical processes. In the past thirty years, attention was drawn to ZSM-5 and other silicon-rich zeolites (with

Si/Al > 12). Their protonic forms are currently used as acid catalysts for hydrocarbon transformations in petrochemistry<sup>1-4</sup> and they are regarded to be promising catalysts for synthesis of fine chemicals<sup>5-8</sup> and for transformation of biomass into chemicals<sup>9,10</sup>. Their transition metal exchanged forms have been discovered as exceptional redox catalysts for nitrogen oxide abatement<sup>11,12</sup>, and a selective oxidation of hydrocarbons by nitrous oxide<sup>13</sup>.

The species assumed to be the active sites in the mentioned reactions, i.e. protons, metal ions and metal-oxo species, are positively charged and compensate the negatively charged aluminosilicate framework. Therefore the Al siting in zeolite frameworks governs the location of the active sites as well as their properties. This is important for both the acid catalyzed hydrocarbon syntheses<sup>14</sup> as well as redox reactions<sup>15,16</sup>. Thus, the Al siting in zeolites is of crucial importance for their catalytic behavior.

In this paper, the siting of Al atoms over the individual T sites of the Theta-1 and ZSM-22 zeolites (both having the framework of the TON structure) is examined employing a combination of our calculations and already published results of <sup>27</sup>Al 3Q MAS NMR experiments<sup>17</sup>. Zeolites with the TON structure represent one-dimensional analogues of the ZSM-5 zeolite which is the most industrially important silicon-rich zeolite. The TON structure is thus frequently used as material for a comparison in detailed studies of catalytic processes over ZSM-5 catalysts.

The predictions of the <sup>27</sup>Al isotropic chemical shifts corresponding to Al in the individual T sites are based on DFT calculations of the local structures of the AlO<sub>4</sub><sup>-</sup> tetrahedra employing a quantum mechanics – molecular mechanics hybrid approach (QM-Pot)<sup>18-20</sup>. The subsequent evaluation of the NMR shielding values uses the GIAO method<sup>21</sup>. The calculated Al shieldings were converted to Al isotropic shifts employing the silicon-rich zeolite of chabasite as a secondary standard<sup>20</sup>. The predicted shifts are then compared with the results of <sup>27</sup>Al 3Q MAS NMR measurements<sup>17</sup>. Good agreement between the calculated and observed <sup>27</sup>Al isotropic chemical shifts is found and two assignments of the observed resonances to the T sites of TON are made.

Further the effect of a silanol “nest” as a next-next-nearest neighbor on the local Al geometry as well as the <sup>27</sup>Al isotropic chemical shift was computationally investigated.

## METHODS

### *Computational Model*

The computations are performed for a single Al atom in a unit cell of Theta-1. A bare zeolite framework model that includes neither cations nor water molecules and has proven useful in our previous study<sup>20</sup> is adopted to calculate the local structure around the  $\text{AlO}_4^-$  tetrahedra and to predict the  $^{27}\text{Al}$  NMR shielding. The starting structure was generated from an X-ray structure of the Theta-1 zeolite<sup>22</sup>.

### *Optimization of Structures*

Both the lattice constants and the atomic positions of the all-silica TON structure were optimized at constant pressure by the GULP program<sup>23,24</sup> using interatomic potential functions only. Then the silicon atom in the site of interest was replaced by an aluminum atom, and the structure and the lattice constants were further optimized at constant pressure. The optimized structure was subsequently used for defining a cluster around the Al atom for our QM-Pot calculations<sup>18,19</sup>. The clusters were embedded into a super cell composed of eight unit cells of the zeolite framework and the structure of the entire system was optimized by QMPOT at constant volume.

To model the effect of the presence of a silanol "nest" on the  $^{27}\text{Al}$  isotropic chemical shift, the silicon atom in the site of interest was removed and the dangling bonds of the four O atoms were terminated by hydrogen atoms. The lattice parameters and atom positions were optimized by GULP at constant pressure employing interatomic potential functions. The optimized structure was then utilized to prepare a cluster around both the Al atom and the hole (missing Al atom). The clusters were embedded into twenty unit cells and optimized by QMPOT at constant volume.

### *Cluster Models*

To calculate the structure of  $\text{AlO}_4^-$  tetrahedra for Al accommodating each of the six T sites of a unit cell of TON, clusters having the Al atom in the center and including five coordination shells ( $\text{Al-O-Si-O-Si-O-H}_{\text{link}}$ ) were used<sup>20,25</sup>. Furthermore clusters containing  $\text{Al-O-Si(1)-O-Si(2)-OH}_{(\text{silanol "nest"})}$  sequences were employed to investigate the effect of a silanol "nest" as a next-next-nearest neighbor on the local Al geometry as well as the  $^{27}\text{Al}$  iso-

tropic chemical shift. The clusters were prepared by merging two five coordination shell clusters which were centered around the Al atom and the hole (missing Al atom). The clusters were cut out from the corresponding optimized super cells. Due to the presence of silicate rings in the zeolite framework, the created five-shell clusters contained pairs of very close  $H_{\text{link}}$  atoms. Since the close  $H_{\text{link}}$  atoms represented the same Si atom, they were replaced by the corresponding  $\text{Si}(\text{OH}_{\text{link}})_2$  moiety. This was repeated until the cluster contained no such pairs.

Our calculations of the  $\text{Al-O-Si(1)-O-Si(2)-OH}_{\text{(silanol "nest")}}$  sequences were performed for two variants of the corresponding cluster for each structure. The first variant contains a silanol "nest"  $\text{Al-O-Si(1)-O-Si(2)-OH}_{\text{(silanol "nest")}}$  while the second variant includes the TON structure without this defect ( $\text{Al-O-Si(1)-O-Si(2)-O-Si(3)}$ ; for these structures the clusters are centered around the Al and Si(3) atoms). This allows comparing the calculated Al local geometry and  $^{27}\text{Al}$  chemical shift using the clusters of the same shape and number of coordination shells.

### *QM-Pot Method and Programs Used*

The QM-Pot method employed<sup>18,19</sup> partitions the whole system (S) into two parts. The inner part (I) is treated by quantum mechanics (QM) and the outer part (O) as well as all the interactions between the inner and outer layers are treated by parametrized interatomic potential functions (Pot). The dangling bonds of the inner part are saturated by link hydrogen atoms. The atoms of the inner part together with the link atoms form the cluster (C). The QM-Pot energy of the whole system is given by

$$E^{\text{QM-Pot}}(\text{S}) = E^{\text{QM}}(\text{C}) + E^{\text{Pot}}(\text{S}) - E^{\text{Pot}}(\text{C})$$

where  $E^{\text{QM}}(\text{C})$  is the energy of the cluster at the QM level,  $E^{\text{Pot}}(\text{S})$  is the energy of the entire system at the Pot level and  $E^{\text{Pot}}(\text{C})$  is the energy of the cluster at Pot. The QM-Pot approach is discussed in detail elsewhere<sup>26</sup>.

The calculations were performed by the QMPOT program<sup>19</sup> which utilizes the Turbomole program<sup>27-31</sup> for the QM part and the GULP program<sup>23,24</sup> for the periodic potential function calculations. The pure DFT method employing the BLYP<sup>32-34</sup> functional and the TZVP basis set of Ahlrichs<sup>35</sup> were used for the QM calculations. As interatomic potential functions (Pot), shell-model ion-pair potentials<sup>36</sup> parametrized on DFT results for zeolites<sup>37</sup>

were employed. The electrostatic energy was evaluated by standard Ewald summation techniques for all cores and shells. A cut-off radius of 10 Å was chosen for the summation of short-range interactions.

### *Calculation of $^{27}\text{Al}$ Isotropic Chemical Shifts*

Subsequently to the QM-Pot structure determination, the Gaussian program<sup>38</sup> was employed to calculate NMR shielding tensors of the atoms of the optimized clusters at the BLYP/TZVP level using the Gauge-Independent Atomic Orbital method (GIAO)<sup>21</sup>.

The NMR shieldings of Al accommodating each of the six distinguishable T sites of the TON structure were converted into isotropic chemical shifts employing a chabasite sample having the Si/Al ratio of 38 ( $^{27}\text{Al}$  NMR shielding of 490.0 ppm corresponds to an experimental value of 60.0 ppm for the  $^{27}\text{Al}$  isotropic chemical shift)<sup>20</sup>.

The NMR shieldings of Al in the Al–O–Si(1)–O–Si(2)–OH<sub>(silanol “nest”)</sub> sequences were not converted into isotropic chemical shifts because the clusters of different shapes and sizes were used for different silanol “nests” structures.

## RESULTS AND DISCUSSION

### *Local $\text{AlO}_4$ Structures and $^{27}\text{Al}$ NMR Shieldings*

Our QM-Pot calculations of the TON framework (P1 symmetry) containing one Al atom per unit cell resulted in 6 distinguishable structures corresponding to Al substitution into the 6 T sites of TON. The eightfold T1 and T2 sites split into fourfold sites T1-1, T1-2 and T2-1, T2-2, respectively (Table I). The structure of a unit cell of TON reflecting the splitting of the T1 and T2 sites is shown in Fig. 1. The force field relative energies of Al in the 6 T sites of TON are all within 4.0 kcal/mol, see Table I. The site T2-1 is the most stable, T1-2 is the least stable one.

Table I reveals the calculated four individual T–O–T angles and the average T–O–T angles, the GIAO  $^{27}\text{Al}$  NMR shieldings and the corresponding isotropic chemical shifts (calibrated employing the chabasite zeolite) for the 6 T sites. Note that a higher shielding corresponds to a lower chemical shift. The calculated Al–O–Si angles scatter between 132 and 172°, but the average Al–O–Si angles vary significantly less – from 141 (T3 site) to 148° (T4 site).

Lippmaa et al.<sup>39</sup> suggested a linear correlation between the  $^{27}\text{Al}$  NMR isotropic shift  $\delta(\text{Al})$  and the average T–O–T angle ( $\theta$ ) of the zeolite framework based on the crystallographic and  $^{27}\text{Al}$  NMR data of aluminum-rich zeolites.

$$\delta(\text{Al}) = -0.50 * \theta + 132 \text{ (ppm)}$$

TABLE I

Force field relative energies (kcal/mol) of Al in the T sites of TON, BLYP GIAO  $^{27}\text{Al}$  NMR shieldings (ppm) and isotropic chemical shifts<sup>a</sup> (ppm), Al–O–Si and average Al–O–Si angles (°) for the individual T sites of TON

T site	Multiplicity	Energy	Shielding	Shift	T–O–T Angle			Average	
T1-1	4	1.5	488.9	61.1	133.3	136.1	141.1	153.5	141.0
T1-2	4	4.0	488.4	61.6	132.2	133.0	139.8	172.1	144.3
T2-1	4	0.0	490.4	59.6	139.4	140.4	144.4	147.5	142.9
T2-2	4	3.1	490.2	59.8	140.1	140.9	143.6	143.8	142.1
T3	4	2.2	489.5	60.5	137.6	138.2	141.5	145.6	140.7
T4	4	3.8	494.7	55.3	139.2	143.0	146.1	165.3	148.4

<sup>a</sup> The  $^{27}\text{Al}$  NMR isotropic shifts were obtained by a conversion of the BLYP GIAO shieldings using the calculated and measured shielding/shift values 490.0 and 60.0 ppm, respectively, for the chabasite sample (Si/Al = 38).

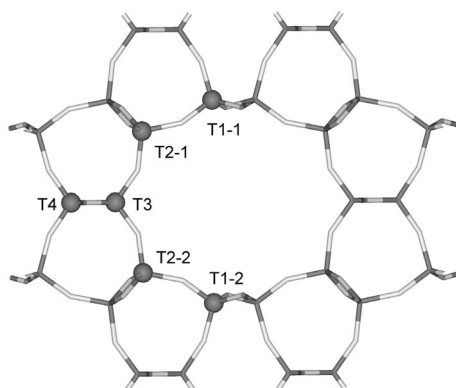


FIG. 1

The structure of a unit cell of TON reflecting the splitting of the T1 and T2 sites

The calculated GIAO  $^{27}\text{Al}$  NMR shifts of TON are plotted against the average Al–O–Si angles in Fig. 2. The plot shows that the linear correlation does not hold even when the calculated Al–O–Si angles are used instead of crystallographic T–O–T angles. The same conclusion has been achieved for ZSM-5<sup>20</sup>.

### *Assignments of Observed Resonances to T Sites and Aluminum Distribution in TON*

The results of single pulse  $^{27}\text{Al}$  NMR experiments revealed that during the calcination of the as-made ZSM-22 and Theta-1 samples a part of the framework Al became octahedral<sup>17</sup>. This makes a comparison of the experimental data on the calcined samples and our calculations impossible due to an unknown effect of the octahedral framework Al on other Al tetrahedral atoms. The octahedral framework Al atoms transform back to tetrahedral Al after ion-exchange. Therefore we compare our calculated  $^{27}\text{Al}$  isotropic chemical shifts only with experimental results obtained for ion-exchanged samples<sup>17</sup>.

Figure 3 shows the calculated and measured (for the ion-exchanged sample)  $^{27}\text{Al}$  isotropic chemical shifts for Theta-1<sup>17</sup>. The values for the six T sites extend over ranges of 6.3 and 3.2 ppm, respectively. Note that Al can occupy only some T sites in the Theta-1 sample and therefore the calculated shift extension can be significantly larger than the measured one. Based on

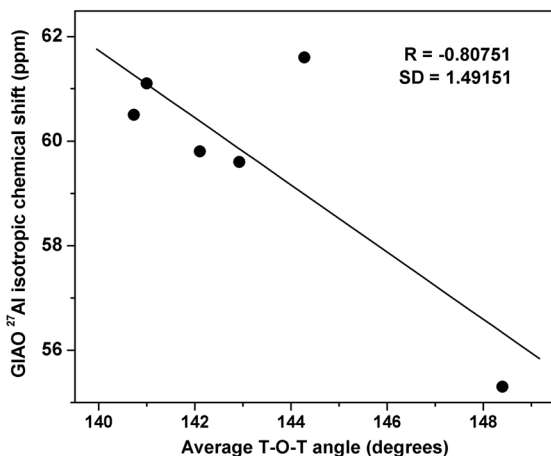


FIG. 2  
 $^{27}\text{Al}$  isotropic shifts plotted against the average T–O–T angles for the 6 T sites of TON

a comparison of the calculated and measured shifts (Fig. 3) there are two plausible assignments. The observed resonance at 55.5 ppm corresponds to T4 for both the assignments. It then follows that the measured resonances at 57.6 and 58.7 ppm belong to T2 (T2-1 or T2-2) and T3, respectively (Assignment 1). It is also possible that the two resonances correspond only to T2 (T2-1 and T2-2), see Fig. 3 (Assignment 2). The calculated  $^{27}\text{Al}$  isotropic chemical shifts of the T2-1 and T2-2 sites are much closer to each other (59.6 and 59.8 ppm, respectively) than those of the two observed resonances (57.6 and 58.7 ppm). A similar feature was observed for resonances R-II (52.9 ppm) and R-III (53.7 ppm) of ZSM-5 which were assigned to T8 (53.3 ppm) and T4 (53.4 ppm), respectively<sup>20</sup>. The calculated shift ranges are 5.2 and 4.5 ppm for Assignments 1 and 2, respectively. These values are closer to the observed shift extension of 3.2 ppm than the entire theoretical shift range of 6.3 ppm since the T1 site of TON is not occupied by Al in the Theta-1 sample used<sup>17</sup>.

Our two assignments are significantly different than those<sup>17</sup> based on Lippmaa correlation<sup>39</sup>. The reason is that the relationship between the  $^{27}\text{Al}$  NMR isotropic shift  $\delta(\text{Al})$  and the average T-O-T angle ( $\theta$ ) employed in ref.<sup>17</sup> does not hold. Moreover, the T-O-T angles employed<sup>17</sup> corresponded to Si-O-Si angles rather than Al-O-Si ones which significantly differ.

Our computational results together with the outcome of the  $^{27}\text{Al}$  single pulse MAS NMR experiments<sup>17</sup> allow to quantify the Al distribution in the

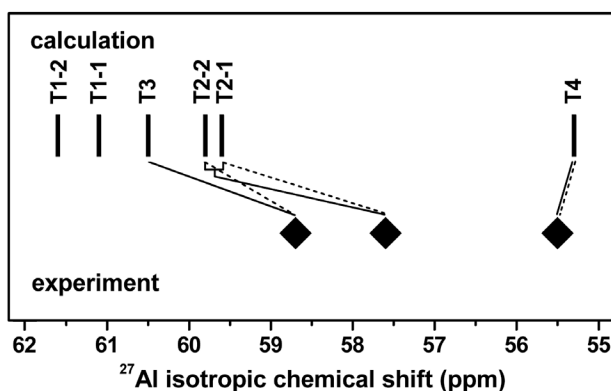


FIG. 3

Comparison of the observed and theoretical  $^{27}\text{Al}$  isotropic chemical shifts of Theta-1; Assignment 1 (—) and Assignment 2 (---)



Theta-1 and ZSM-22 samples. About 55% of the framework Al in Theta-1 (60% in ZSM-22) occupy the T4 site. The remainder (40%) of Al in ZSM-22 populates the T2 site. For the Theta-1 zeolite, 35% of the framework Al locate in T2 (T2-1 or T2-2) and 10% in T3 (Assignment 1) or all the remaining framework Al atoms (45%) occupy T2 (T2-1 and T2-2) (Assignment 2). However, different parameters of the synthesis of the TON zeolite can result in different Al distributions as observed for ZSM-5<sup>20</sup>.

The Al atoms in the most populated T4 site are located in a position which is not on the surface of the TON ten-membered ring channel (see Fig. 1). Thus the protonic sites balancing the negative charge of these  $\text{AlO}_4^-$  tetrahedra correspond to a restricted reaction space and therefore their role as catalytic centers is limited. The "effective" concentration of protonic sites is thus less than one half of the nominal concentration. Moreover, the preference of Al atoms to accommodate the "buried" T4 site indicates that large blocks as  $\text{AlO}_4^-(\text{SiO}_4)_4$  with the  $\text{AlO}_4^-$  tetrahedron surrounded by  $\text{SiO}_4$  tetrahedra are building units during the syntheses of the Theta-1 and ZSM-22 zeolites of the TON structure.

The assignment of individual resonances to Al T sites further allows suggesting the siting of the octahedral framework Al atoms of the calcined Theta-1 and ZSM-22 samples. It was shown<sup>17</sup> that the octahedral framework Al atoms were formed in ZSM-22 on the expense of the tetrahedral Al atoms characterized by an isotropic chemical shift of 55.1 ppm (60% of all Al atoms in the ion-exchanged sample, 12% in the calcined one). Our calculations revealed that the resonance at 55.1 ppm corresponds to Al in the T4 site. The presence of Al in the T4 site is necessary but not sufficient in order for the transformation of the tetrahedral to octahedral framework Al atom to occur (compare the <sup>27</sup>Al NMR isotropic chemical shifts for ZSM-22 and Theta-1). It is not clear whether it is the aluminum content and/or other parameters connected with the increased concentration of Al atoms in the framework of ZSM-22 zeolite compared to Theta-1, e.g. a formation of Al-O-(Si-O)<sub>2</sub>-Al sequences.

#### *Effect of the Presence of Si-OH "Nests" on the <sup>27</sup>Al Isotropic Chemical Shift*

For ZSM-22, a small part of Al atoms was released from their framework positions during the calcination procedure and these Al atoms are present in the zeolite as extraframework Al species, as evidenced by the presence of a broad weak band at around -8 ppm in the <sup>27</sup>Al MAS NMR spectrum of ion-exchanged sample<sup>17</sup>. Silanol "nests" of four terminal Si-OH groups are formed at this Al vacancy in the ZSM-22 framework. These silanol "nests"

are known also for other zeolites and they can significantly affect both the structure and properties of dealuminated zeolites<sup>40-43</sup>.

The ZSM-22 <sup>27</sup>Al NMR signals are observed as broad bands centered at 55.1 and 57.6 ppm. Furthermore there is also present a shoulder centered under 55.1 ppm in the spectrum.

To investigate the effect of the presence of a silanol "nest" as a next-next-nearest neighbor on the <sup>27</sup>Al isotropic chemical shift of Al located in the T4 site, we calculated selected Al(T4)-O-Si(1)-O-Si(2)-OH<sub>(silanol "nest")</sub> sequences. Such sequences are a result of a release of Al from the TON framework. The computational results revealed a small effect of  $\pm 1$  ppm (Table II) which is in agreement with the observed broadening of the <sup>27</sup>Al NMR bands and with the presence of the shoulder in the <sup>27</sup>Al NMR spectrum of the ion-exchanged ZSM-22 sample. Also the calculated change of the average T-O-T angles was tiny (less than 1°). The effect of the presence of a silanol "nest" as a next-nearest neighbor (Al(T4)-O-Si-OH<sub>(silanol "nest")</sub>) was not calculated since the <sup>29</sup>Si MAS NMR spectra of ion-exchanged ZSM-22 and Theta-1 samples revealed no Al-O-Si-O-Al sequences in the zeolite framework<sup>17</sup>. Al-O-Si-O-Al is the precursor of Al(T4)-O-Si-OH<sub>(silanol "nest")</sub>.

TABLE II  
BLYP GIAO <sup>27</sup>Al NMR shieldings (ppm), Al-O-Si and average Al-O-Si angles (°) for Al-O-Si-O-Si-OH sequences

Sequence	Shielding	$\Delta$	T-O-T Angle				Average	$\Delta$
Al-Si-Si-Si (T1-2)	493.1		137.7	141.0	143.6	165.0	146.8	
Al-Si-Si-OH (T1-2)	492.6	-0.5	138.8	140.4	144.1	161.4	146.2	-0.6
Al-Si-Si-Si (T3)	494.9		140.4	142.4	147.8	163.0	148.4	
Al-Si-Si-OH (T3)	495.6	0.7	142.4	142.6	148.3	162.6	149.0	0.6
Al-Si-Si-Si (T3)	494.0		140.3	142.1	147.3	157.5	146.8	
Al-Si-Si-OH (T3)	493.2	-0.8	137.2	142.2	144.3	160.5	146.1	-0.7

## CONCLUSIONS

Our QM-Pot calculations of the TON framework (Si/Al = 23) resulted in six distinguishable structures corresponding to Al substitution into the 6 T sites of TON and six <sup>27</sup>Al NMR shieldings. The two eightfold T1 and T2 sites split into four fourfold sites: T1-1, T1-2 and T2-1, T2-2, respectively. Based on our calculations and experimental results of Derewinski we show that at

least 2 and 3 out of 6 distinguishable framework T sites are occupied by Al atoms in the ZSM-22 and Theta-1 zeolites, respectively. The observed  $^{27}\text{Al}$  isotropic shift of 55.5 ppm for Theta-1 (55.1 ppm for ZSM-22) corresponds to Al atoms in the T4 site. There are two plausible assignments of the  $^{27}\text{Al}$  NMR signals centered at 57.6 ppm (Theta-1 and ZSM-22) and 58.7 ppm (Theta-1 only). The former and latter relate to T2 (T2-1 or T2-2) and T3, respectively, or only to T2 (T2-1 and T2-2). Al atoms in the T4 site predominate in the Theta-1 and ZSM-22 zeolites (about 60%). Some 40% of Al atoms are located in the T2 site, and the T3 site accommodates only a minority of Al atoms (10%) or is together with the T1 site unoccupied by Al atoms.

We further show that the octahedral framework Al atoms formed in the protonic form of ZSM-22 are most likely located in the T4 site. The calculated effect of the presence of a silanol "nest" as a next-next-nearest neighbor on the  $^{27}\text{Al}$  isotropic chemical shift of Al located in the T4 site is modest ( $\pm 1$  ppm).

*This work was financially supported by the Czech Science Foundation (Project No. 203/06/1449).*

## REFERENCES

1. Bellussi G., Pazzuconi G., Perego C., Girotti G., Terzoni G.: *J. Catal.* **1995**, *157*, 227.
2. Čejka J., Wichterlová B.: *Catal. Rev.–Sci. Eng.* **2002**, *44*, 375.
3. Chang C. D.: *Catal. Rev.–Sci. Eng.* **1983**, *25*, 1.
4. Corma A., Martinez A.: *Catal. Rev.–Sci. Eng.* **1993**, *35*, 483.
5. Climent M. J., Corma A., Iborra S.: *J. Catal.* **2005**, *233*, 308.
6. Corma A.: *Chem. Rev.* **1995**, *95*, 559.
7. Corma A., Fornes V., Pergher S. B., Maesen T. L. M., Buglass J. G.: *Nature* **1998**, *396*, 353.
8. Sartori G., Maggi R.: *Chem. Rev.* **2006**, *106*, 1077.
9. Corma A., Iborra S., Velty A.: *Chem. Rev.* **2007**, *107*, 2411.
10. Huber G. W., Iborra S., Corma A.: *Chem. Rev.* **2006**, *106*, 4044.
11. Shelef M.: *Chem. Rev.* **1995**, *95*, 209.
12. Yahiro H., Iwamoto M.: *Appl. Catal., A* **2001**, *222*, 163.
13. Panov G. I., Kharitonov A. S., Sobolev V. I.: *Appl. Catal., A* **1993**, *98*, 1.
14. Csicsery S. M.: *Pure Appl. Chem.* **1986**, *58*, 841.
15. Armor J. N.: *Microporous Mesoporous Mater.* **1998**, *22*, 451.
16. Wichterlová B., Sobalík Z., Dědeček J.: *Appl. Catal., B* **2003**, *41*, 97.
17. Derewinski M., Sarv P., Mifsud A.: *Catal. Today* **2006**, *114*, 197.
18. Eichler U., Kolmel C. M., Sauer J.: *J. Comput. Chem.* **1997**, *18*, 463.
19. Sierka M., Sauer J.: *J. Chem. Phys.* **2000**, *112*, 6983.
20. Sklenak S., Dědeček J., Li C. B., Wichterlová B., Gábová V., Sierka M., Sauer J.: *Angew. Chem. Int. Ed.* **2007**, *46*, 7286.
21. Wolinski K., Hinton J. F., Pulay P.: *J. Am. Chem. Soc.* **1990**, *112*, 8251.

22. Papiz Z., Andrews S. J., Damas A. M., Harding M. M., Highcock R. M.: *Acta Crystallogr., Sect. C: Cryst. Struct. Commun.* **1990**, *46*, 172.
23. Gale J. D., Rohl A. L.: *Mol. Simul.* **2003**, *29*, 291.
24. Gale J. D.: *J. Chem. Soc., Faraday Trans.* **1997**, *93*, 629.
25. Bussemer B., Schroder K. P., Sauer J.: *Solid State Nucl. Magn. Reson.* **1997**, *9*, 155.
26. Brandl M., Sauer J.: *J. Am. Chem. Soc.* **1998**, *120*, 1556.
27. Eichkorn K., Treutler O., Ohm H., Haser M., Ahlrichs R.: *Chem. Phys. Lett.* **1995**, *242*, 652.
28. Eichkorn K., Treutler O., Ohm H., Haser M., Ahlrichs R.: *Chem. Phys. Lett.* **1995**, *240*, 283.
29. Eichkorn K., Weigend F., Treutler O., Ahlrichs R.: *Theor. Chem. Acc.* **1997**, *97*, 119.
30. Haser M., Ahlrichs R.: *J. Comput. Chem.* **1989**, *10*, 104.
31. Treutler O., Ahlrichs R.: *J. Chem. Phys.* **1995**, *102*, 346.
32. Becke A. D.: *Phys. Rev. A* **1988**, *38*, 3098.
33. Lee C. T., Yang W. T., Parr R. G.: *Phys. Rev. B* **1988**, *37*, 785.
34. Miehlich B., Savin A., Stoll H., Preuss H.: *Chem. Phys. Lett.* **1989**, *157*, 200.
35. Schafer A., Huber C., Ahlrichs R.: *J. Chem. Phys.* **1994**, *100*, 5829.
36. Catlow C. R. A., Dixon M., Mackrodt W. C.: *Lect. Notes Phys.* **1982**, *166*, 130.
37. Sierka M., Sauer J.: *Faraday Discuss.* **1997**, *106*, 41.
38. Frisch M. J., Trucks G. W., Schlegel H. B., Scuseria G. E., Robb M. A., Cheeseman J. R., Montgomery J. A., Jr., Vreven T., Kudin K. N., Burant J. C., Millam J. M., Iyengar S. S., Tomasi J., Barone V., Mennucci B., Cossi M., Scalmani G., Rega N., Petersson G. A., Nakatsuji H., Hada M., Ehara M., Toyota K., Fukuda R., Hasegawa J., Ishida M., Nakajima T., Honda Y., Kitao O., Nakai H., Klene M., Li X., Knox J. E., Hratchian H. P., Cross J. B., Bakken V., Adamo C., Jaramillo J., Gomperts R., Stratmann R. E., Yazyev O., Austin A. J., Cammi R., Pomelli C., Ochterski J. W., Ayala P. Y., Morokuma K., Voth G. A., Salvador P., Dannenberg J. J., Zakrzewski V. G., Dapprich S., Daniels A. D., Strain M. C., Farkas O., Malick D. K., Rabuck A. D., Raghavachari K., Foresman J. B., Ortiz J. V., Cui Q., Baboul A. G., Clifford S., Cioslowski J., Stefanov B. B., Liu G., Liashenko A., Piskorz P., Komaromi I., Martin R. L., Fox D. J., Keith T., Al-Laham M. A., Peng C. Y., Nanayakkara A., Challacombe M., Gill P. M. W., Johnson B., Chen W., Wong M. W., Gonzalez C., Pople J. A.: *Gaussian03*, Revision C.02, 2004. Gaussian, Inc., Wallingford (CT) 2004.
39. Lippmaa E., Samoson A., Magi M.: *J. Am. Chem. Soc.* **1986**, *108*, 1730.
40. Dessau R. M., Schmitt K. D., Kerr G. T., Woolery G. L., Alemany L. B.: *J. Catal.* **1987**, *104*, 484.
41. Engelhardt G., Lohse U., Samoson A., Magi M., Tarmak M., Lippmaa E.: *Zeolites* **1982**, *2*, 59.
42. Sokol A. A., Catlow C. R. A., Garces J. M., Kuperman A.: *J. Phys. Chem. B* **2002**, *106*, 6163.
43. Vannierkerk M. J., Fletcher J. C. Q., Oconnor C. T.: *J. Catal.* **1992**, *138*, 150.